

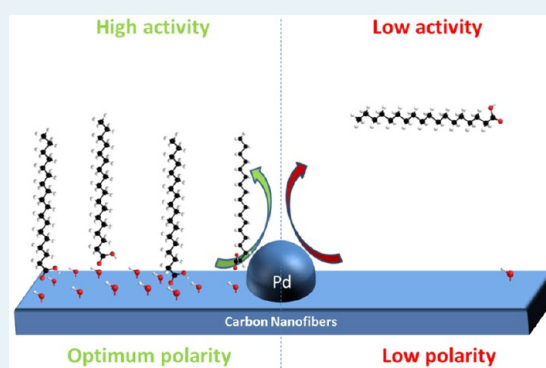
Enhancing the Activity of Pd on Carbon Nanofibers for Deoxygenation of Amphiphilic Fatty Acid Molecules through Support Polarity

R. W. Gosselink, W. Xia, M. Muhler, K. P. de Jong, and J. H. Bitter*

Department of Inorganic Chemistry and Catalysis, Utrecht University, Universiteitsweg 99, 3584CG, Utrecht, The Netherlands

ABSTRACT: The influence of support polarity on Pd/CNF for the deoxygenation of fatty acids was studied. Catalysts with a low ($O/C = 3.5 \times 10^{-2}$ at/at from X-ray photoelectron spectroscopy (XPS)) and a high ($O/C = 5.9 \times 10^{-2}$ at/at from XPS) amount of oxygen containing groups on the support were prepared. The latter were introduced via a HNO_3 gas phase oxidation treatment on Pd loaded supports. The presence of oxygen containing groups was beneficial for the activity of Pd for the deoxygenation of the amphiphilic stearic acid. This is attributed to a favorable mode of adsorption of the reactant via the carboxylic acid group on the more polar support in the vicinity of the catalytically active Pd nanoparticles.

KEYWORDS: carbon nanofibers, deoxygenation, support polarity, adsorption effect, fatty acids



1. INTRODUCTION

Supported heterogeneous catalysts consist of an active phase (e.g., metal, metal oxide, metal sulfide, protons), a support, and optionally one or more promoters. Though the catalytic reaction itself takes place on the active phase the support is not always a spectator in the reaction network. For example Bitter et al. showed that for CO_2/CH_4 reforming over Pt/ ZrO_2 CO_2 adsorption on the support was essential for a high activity. The reaction was claimed to take place on the metal–support perimeter.¹ Toebe et al. provided evidence that a high amount of cinnamaldehyde adsorbed on the support is beneficial for the cinnamaldehyde hydrogenation over Pt/CNF catalysts.² The amount of adsorbed reactant was increased by lowering the polarity of the carbon support. Wang et al. showed that polarity of the support plays an important role for the aqueous phase reforming of ethylene glycol over Pt/CNT.³ A too high polarity leads to the competitive adsorption between water and ethylene glycol resulting in a low catalytic activity.

The above-mentioned examples indicate that the support can play a key role in catalysis by adsorbing reactants. Therefore tuning the sorption properties of a support is a tool to steer catalysis.

Adsorption properties of a catalyst (support) are related to the support textural properties and chemical composition. Carbon, especially mesoporous carbon nanotubes (CNT) and carbon nanofibers (CNF), is an eminently suitable support material for studying adsorption effects in catalysis. For these materials the sorption properties can be modified by introducing or removing surface oxygen- or nitrogen containing groups resulting in supports varying in polarity and chemical composition.^{3,4}

The influence of support polarity on CNF has been investigated for various reactions, such as the above-mentioned selective hydrogenation of cinnamaldehyde^{2,5} and the oxidation of benzyl alcohol.⁶ It has been reported that the presence of oxygen containing groups on the support is detrimental for the selective hydrogenation of cinnamaldehyde catalyzed by Pt/CNF.² To reach that conclusion the authors first prepared a Pt/CNF catalyst with an O/C atomic ratio of 4.5×10^{-2} based on X-ray photoelectron spectroscopy (XPS). Heat treatments were subsequently applied to decrease the amount of oxygen containing groups on the support; the lower limit was an O/C atomic ratio of 1.2×10^{-2} as determined by XPS. As a result, the hydrogenation activity was enhanced by a factor of 2 to 25, depending on the applied reaction conditions.^{2,5} The increased activity has been ascribed to a preferred mode of adsorption of the cinnamaldehyde at an apolar support (low oxygen content), resulting in facilitated hydrogenation.

Conversely, Tang et al. has shown that oxygen containing groups on the support can have a beneficial influence on catalysis for a different reaction, that is, the oxidation of benzyl alcohol catalyzed by Ru/CNF.⁶ In parallel to the work of Toebe et al.² the amount of oxygen containing groups was decreased by applying a heat treatment. As a result, a decrease in benzyl alcohol conversion with a factor of 2 is reported. It has been claimed that the oxygen containing groups on the support repel the benzyl group of the reactant and activate the

Received: June 26, 2013

Revised: September 2, 2013

Published: September 9, 2013

alcohol group, thereby assisting the oxidation of the benzyl alcohol if this occurs in the vicinity of Ru.

In both examples, the influence of oxygen containing groups on the reaction has thus been related to the preferential adsorption of an amphiphilic reactant. This is ascribed to an interaction of the polar or apolar part of the molecule with the support. Here we will investigate the role of oxygen containing groups on Pd/CNF for the deoxygenation of fatty acids, which are clearly amphiphilic in nature, that is, a polar carboxylic group and an apolar hydrocarbon tail. This reaction was chosen as show case for biomass related deoxygenation reactions.

Because of the increasing energy consumption and environmental concern, vegetable oil/fat and fatty acid based feeds are considered as alternative resources for energy carriers and precursors for bulk chemicals.^{7–10} A disadvantage, however, is the high oxygen content in these feedstocks which makes the feed inapplicable in current existing processes. Deoxygenation of these feeds yields alkanes and alkenes which are compatible with the currently available infrastructure and processes.

Several studies have been performed on the catalytic deoxygenation of fatty acids.^{11–14} From these studies it can be concluded that Pd is the most active metal for this reaction and activated carbon (AC) the most preferred support.¹¹

We hypothesize that the polarity of the carbon support can also influence the deoxygenation of fatty acids because of the amphiphilic nature. Therefore the role of oxygen containing groups on a CNF support for this reaction is investigated in this study.

As has been shown in the examples above, the oxygen content is mostly varied by decreasing the oxygen content of the parent material via the decomposition of oxygen containing groups. As a result, only catalysts with relatively low polarities can be compared, as the “highly” polar support had an O/C atomic ratio of 4.5×10^{-2} as determined by XPS. We have recently reported a method to introduce oxygen containing groups onto metal-loaded CNF by Gas phase Oxidation (GPO) using HNO₃ vapor. XPS revealed that we could increase the O/C atomic ratio to 7.6×10^{-2} , with minimal impact to the Pd particle size.¹⁵ As a result, we are now able to include catalysts with significantly higher oxygen contents in our study as compared to previous work.

In the current study GPO is used as a tool to introduce oxygen containing groups on CNF to gain fundamental insight into the role of the support polarity in the deoxygenation of stearic acid. Catalysts are prepared with a low oxygen content by applying heat treatments and high oxygen content by performing GPO on CNF supported Pd catalysts.

2. EXPERIMENTAL SECTION

CNF Growth. A 5 wt % Ni/SiO₂ growth catalyst was prepared by homogeneous deposition-precipitation as reported previously.^{2,5} Fishbone type CNFs were subsequently obtained by flowing a CO/H₂/N₂ mixture (266/102/450 mL/min) at 3 bar overpressure over 5 g of reduced Ni/SiO₂ at 550 °C for 24 h. The raw product was collected and refluxed three times in boiling 1.0 M KOH, with intermediate washing using deionized water, to remove SiO₂. Finally, the fibers were treated with boiling, concentrated HNO₃ for 1.5 h to remove exposed nickel and introduce oxygen containing groups. This sample was denoted as CNF-ox.

Palladium Deposition. Prior to impregnation the CNF-ox were dried under vacuum at 100 °C. Palladium was deposited on the CNF-ox (1 g) by pore volume (0.7 mL/g determined by

water uptake) impregnation under vacuum with Pd-(NH₃)₄(NO₃)₂ (10 wt % in water). After impregnation the sample was dried under vacuum at 100 °C for 24 h. Decomposition of the palladium precursor was accomplished by heat treatment under N₂ flow (50 mL/min) at 200 °C for 2 h. This sample was denoted as Pd/CNF-ox. Hereafter a subsequent heat treatment was applied at 625 °C (5 °C/min) for 15 min to decompose the oxygen containing groups and simultaneously sinter Pd particles to exclude any particle size effect during further treatments. This sample was denoted as Pd/CNF.

Gas Phase Oxidation (GPO). HNO₃ GPO of Pd/CNF was performed using a similar setup as reported previously.^{15,16} The sample, typically 500 mg, was loaded in a glass reactor with a demountable oven equipped with a reflux condenser on top of the reactor. The sample was first dried at 125 °C for 2 h in static air. Next a one necked flask containing 125 mL of concentrated HNO₃ (65%, Merck) was attached to the oven at an angle to make sure that any liquid returning from the condenser bypassed the sample. The concentrated HNO₃ was heated to 100 °C, and the sample was kept at 125 °C for 15 h. After GPO treatment the oven including the sample was removed from the setup and left for 2 h at 125 °C in air. This sample was denoted as Pd/CNF-O.

Characterization. N₂-physisorption isotherms were recorded with a Micromeritics Tristar 3000 at 77 K after drying the samples for at least 16 h at 200 °C in an N₂ flow.

X-ray powder diffraction (XRD) patterns were obtained using a Bruker-AXS D2 Phaser powder X-ray diffractometer.

The oxygen content was determined by two methods, that is, titration and XPS.¹⁵ Titration was performed using a Titralab TIM 880 titration manager with a solution of 0.1 M KCl and 0.01 M NaOH as a titrant to establish the amount of acidic oxygen containing groups. The titration results are presented in mmol acidic groups per gram.

XPS measurements were carried out in an UHV setup equipped with a Gammatdata-Scienta SES 2002 analyzer. The base pressure in the measurement chamber was 5×10^{-10} mbar. Monochromatic Al K_α (1486.6 eV; 14.5 kV; 45 mA) was used as incident radiation, and a pass energy of 200 eV was chosen resulting in an energy resolution better than 0.5 eV. Charging effects were compensated using a flood gun. Binding energies were calibrated by positioning the main C 1s peak at 284.5 eV. The CASA XPS program with a Gaussian–Lorentzian mix function and Shirley background was used to analyze the XP spectra quantitatively. The peak positions for all the samples were reproducible using a fixed Gaussian to Lorentz ratio of 70:30 and fixed full width at half maximums (FWHMs). Surface atomic concentration was calculated using sensitivity factors provided in ref 17. The XPS results are presented as atomic O/C ratios.

Transmission electron microscopy (TEM) analysis was performed using a FEI TECNAI20F Transmission Electron Microscope operated at 200 KeV. A small amount of the sample was powdered in a mortar for about 1 min in ethanol. Subsequently the sample was treated in an ultrasonic bath for 10 s and then settled for about 1 min. One drop of the ethanol with the small particles was dispersed onto a thin carbon film on a copper grid, followed by the evaporation of the ethanol.

H₂-chemisorption measurements were performed using a Micromeritics ASAP 2020. Samples were dried at 423 K for 60 min (ramp 5 K/min) in vacuum. Subsequently the samples were reduced at 523 K (ramp 5 K/min) for 2 h under H₂ flow.

Hereafter the samples were degassed for 30 min under vacuum at 523 K. Adsorption isotherms were measured at 363 K to avoid the formation of palladium bulk hydrides.

Catalytic Test. The catalytic experiments were carried out in a 75 mL Parr batch reactor. Typically 0.25 g of catalyst (212–425 μm) was activated in 6 bar H_2 at 150 $^\circ\text{C}$ for 2 h. These samples are referred to as Pd/CNF-red and Pd/CNF-O-red. The reactor was flushed with N_2 at 150 $^\circ\text{C}$ to exclude the presence of H_2 in the form of PdH. Hereafter, 1 g of stearic acid (ABCR) in 25 mL of dodecane (Acros) was added under inert conditions. Experiments were then carried out at temperatures ranging from 225 to 275 $^\circ\text{C}$ at 6 bar N_2 pressure, while stirring at 1100 rpm. Spent catalysts were referred to as Pd/CNF-sp and Pd/CNF-O-sp. Reaction mixture work up was performed with a CHCl_3 :MeOH (2:1) mixture that was heated to 40 $^\circ\text{C}$ to ensure complete dissolution of the stearic acid. A sample was subsequently taken from the mixture and methylated using TMSH (Fluka) to analyze by Gas Chromatography (GC).¹⁸

Average turnover frequencies (TOF) were calculated using average particle size as determined from TEM and surface Pd species obtained by H_2 -chemisorption and expressed as $\text{mol C17}/(\text{mol Pd}_{\text{surf}}\text{s})$.

3. RESULTS AND DISCUSSION

Catalyst Characterization. Parent Material - Pd/CNF-ox. The Brunauer–Emmett–Teller (BET) surface area of CNF-ox was 190 m^2/g , with a pore volume of 0.43 cm^3/g . This is in accordance with results previously reported for CNF thus synthesized.^{2,5} TEM revealed the presence of a fishbone fiber structure for CNF-ox with an average diameter of 30 nm. Figure 1 shows a TEM micrograph of Pd/CNF-ox. Pd nanoparticles with an average size of ~ 2 nm are visible as black dots.

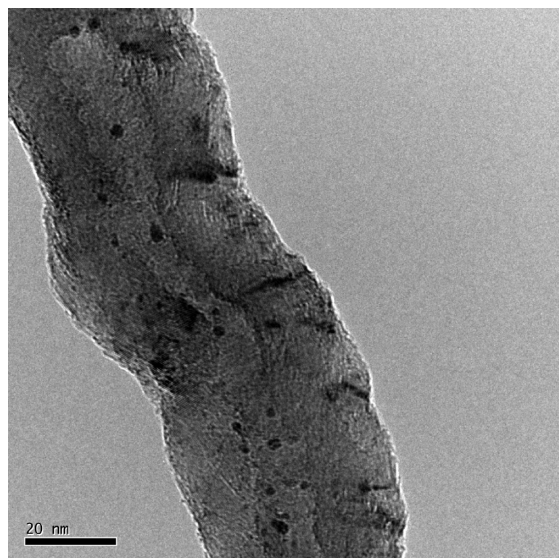


Figure 1. TEM image of the parent Pd/CNF-ox.

Oxygen Content. The O/C atomic ratios, as determined by XPS, for the samples after the different treatments are reported in Table 1 together with the amount of acidic groups in mmol/g. XPS indicated that a heat treatment at 625 $^\circ\text{C}$ on Pd/CNF-ox to yield Pd/CNF resulted in a decrease of the O/C ratio from 5.2×10^{-2} to 3.5×10^{-2} , showing the successful decomposition of a significant amount of oxygen containing

Table 1. Influence of the Heat Treatment at 625 $^\circ\text{C}$, GPO, Reduction, and Reaction on the Pd Particle Size and Oxygen Content

sample	Pd particle size		oxygen content	
	XRD (nm)	TEM (nm)	XPS (O/C $\times 10^{-2}$ at/at)	titration (mmol acidic groups/g)
Pd/CNF-ox		2	5.2	<0.005
Pd/CNF	7	7	3.5	<0.005
Pd/CNF-O	7	8	7.3	0.25
Pd/CNF-red	7	7	3.5	<0.005
Pd/CNF-O-red	6	7	5.9	0.06
Pd/CNF-sp	6	7	3.5	<0.005
Pd/CNF-O-sp	5	6	5.4	<0.005

groups. Titration on the other hand did not reveal any acidic groups for Pd/CNF-ox and Pd/CNF. Bare CNF-ox however exhibits acidic oxygen containing groups;¹⁵ thus, these must have been decomposed during the Pd deposition procedure in line with earlier observations.^{2,5,15}

When treating Pd/CNF using GPO to yield Pd/CNF-O the O/C atomic ratio increased from 3.5×10^{-2} to 7.3×10^{-2} . Titrations revealed the presence of 0.25 mmol acidic groups/g, while it revealed no acidic oxygen containing groups for Pd/CNF. Thus, acidic oxygen containing groups were successfully introduced on the Pd containing samples by the GPO treatment as shown previously.¹⁵

Prior to catalytic testing a reduction treatment is applied, which might result in a lowering of the oxygen content present on Pd/CNF and Pd/CNF-O.¹⁹ To determine the actual oxygen content of the catalyst prior to reaction, XPS and titration analysis were also performed on both Pd/CNF-red and Pd/CNF-O-red. Table 1 shows similar O/C ratios for Pd/CNF and Pd/CNF-red and only a limited decrease in oxygen content on going from Pd/CNF-O to Pd/CNF-O-red. The decrease in oxygen content from Pd/CNF-O to Pd/CNF-O-red is explained by the reduction of acidic (carboxylic) oxygen containing groups present on Pd/CNF-O. These groups decompose at relatively low temperatures (150–500 $^\circ\text{C}$).¹⁹ This is also obvious from our results since titrations indicate a large decrease of the acidic oxygen content from 0.25 to 0.06 mmol/g. Nevertheless, the amount of oxygen containing groups on Pd/CNF-O-red is significantly higher compared to Pd/CNF-red, making these catalysts suitable for studying the influence of support polarity on catalysis.

Effect of Catalyst Treatments on Pd. Applying a heat treatment to a palladium loaded CNF catalyst is known to influence the metal particle size.²⁰ The GPO treatment using HNO_3 can also result in a change in the palladium oxidation state and might impact the morphology of the Pd particle. The influence of the heat treatment and GPO treatment on these parameters is studied by XRD (Figure 2), XPS (Figure 3), and TEM (Figure 4). It has also been shown before that the presence of functional groups in the vicinity of palladium particles can affect the electronic structure of the Pd.²¹ Although this is not expected in our samples because of the relatively large Pd particle size (7 nm), XPS studies will give more insight here as the Pd 3d binding energy is sensitive to the electronic structure of Pd.²¹

Both XRD and TEM show an increase in the palladium particle size from 2 to 7 nm upon the heat treatment at 625 $^\circ\text{C}$, thus going from Pd/CNF-ox to Pd/CNF (Table 1). This is in accordance with the Pd particle size observed by Wagemans et

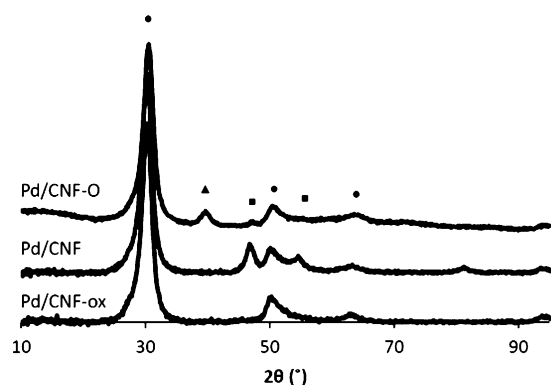


Figure 2. XRD diffractograms of Pd/CNF-ox, Pd/CNF, and Pd/CNF-O. Reflections are given for graphitic carbon (●), Pd (■), and PdO (▲).

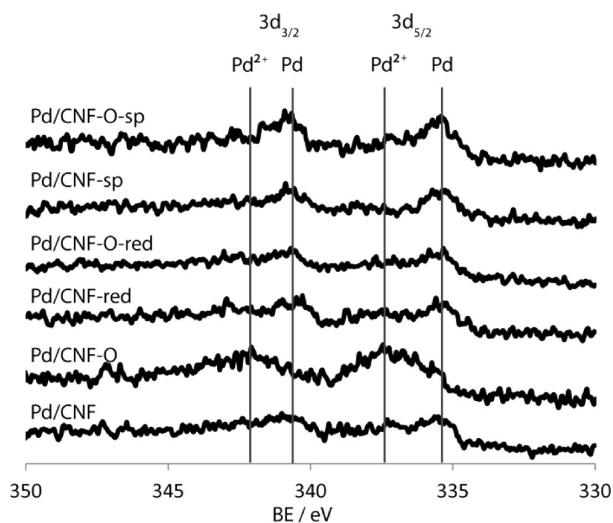


Figure 3. XP spectra of the fresh, activated and spent catalysts.

al.²⁰ A subsequent GPO treatment of 15 h at 125 °C does not significantly affect the Pd particle size any further.¹⁵

XPS in the Pd 3d energy range was used to study the oxidation state and electronic state of the Pd after different treatments (Figure 3). When oxidizing Pd/CNF (to Pd/CNF-O) a clear shift of Pd 3d_{5/2} is observed from 335 to 337 eV and for Pd 3d_{3/2} from 341 to 342 eV, which corresponds to a change in oxidation state from Pd⁰ to Pd²⁺.²² The oxidation of Pd upon a GPO treatment is also evident from XRD (Figure 2), where a clear peak is visible for Pd/CNF-O at 39° 2θ that can be attributed to PdO (corresponding to {101}) while the Pd⁰ diffractions (47 and 54° 2θ) observed for Pd/CNF disappeared. It is shown by XPS that a subsequent reduction

treatment results again in the Pd_{3/2} and Pd_{5/2} peaks characteristic for Pd⁰. According to XPS and XRD, Pd/CNF was already in the Pd⁰ state. Nevertheless, a reductive treatment is applied to keep experimental parameters constant for comparing the catalytic activities. No shift in the Pd 3d binding peaks was observed between Pd/CNF-red and Pd/CNF-O-red.

In Figure 4 representative high-resolution TEM images of Pd/CNF, Pd/CNF-O, Pd/CNF-red, and Pd/CNF-O-red are compiled. For Pd/CNF-O-red, where Pd was present as Pd²⁺, the Pd particle is spherical whereas the Pd⁰ samples show only hemispherical particles. Since the catalysts are always reduced prior to catalytic testing, particles are tested in their hemispherical and identical morphology (Pd/CNF-red and Pd/CNF-O-red).

As such no indications of either structural or electronic changes were obtained by XRD, XPS, and TEM. Thus, any effects of the GPO treatment on catalysis must be related to the impact of oxygen containing groups present on the support.

Catalysis. Deoxygenation experiments of stearic acid were carried out in batch mode at 250 °C using Pd/CNF-red and Pd/CNF-O-red. For both catalysts the deoxygenation of stearic acid is 100% selective to C17 hydrocarbons, that is, only heptadecane (90–99% yield) and heptadecene (1–10% yield) were observed. Heptadecane is the decarboxylation product of stearic acid, whereas heptadecene can be formed via decarbonylation.^{10,23}

The product yield as function of reaction time is presented in Figure 5. Clearly the product yield is significantly higher (about

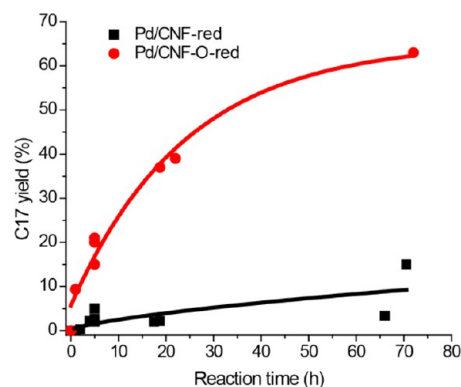


Figure 5. C17 yield of the deoxygenation of stearic acid by Pd/CNF-red and Pd/CNF-O-red. $T = 250$ °C, $P = 6$ bar N₂, $m_{\text{stearic acid}} = 1$ g, $m_{\text{cat}} = 0.25$ g, $m_{\text{dodecane}} = 18$ g.

five times) over Pd/CNF-O-red compared to Pd/CNF-red. Thus the presence of oxygen containing groups on the support is beneficial for the deoxygenation reaction rate.

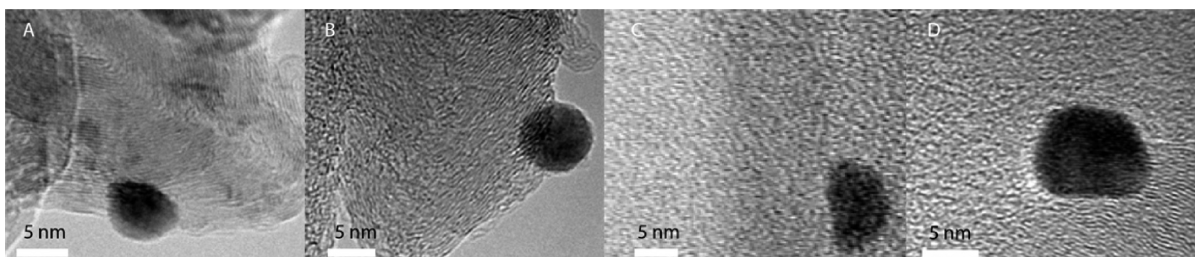


Figure 4. TEM micrographs of Pd/CNF (a), Pd/CNF-O (b), Pd/CNF-red (c), Pd/CNF-O-red (d).

The catalyst particle sizes (212–425 μm) might induce intraparticle mass transfer limitations. To determine this the Weisz–Prater criterion was calculated, with diffusion coefficient for stearic acid as calculated by Smits et al.²⁴ Values of 0.69×10^{-3} and 0.17×10^{-3} were obtained for catalyst particle sizes of 425 and 212 μm , respectively. This indicates the absence of diffusion limitations. This is in agreement with experiments performed with powdered samples ($<90 \mu\text{m}$), which showed no differences in activities and thereby validated the use of these particle sizes.

Reported activity for the deoxygenation of fatty acids varies significantly. This is most likely related to the different reaction temperatures and different carbon supports used.^{24–26} A 5 wt % Pd/C catalyst is reportedly one of the most active catalysts for this reaction.¹¹ We tested this catalyst under identical reaction conditions as given in this paper. An average TOF during the first hour of reaction of 4.0×10^{-2} was obtained which is a factor 4 higher than the average TOF of our catalyst, 1.0×10^{-2} mol C17/(mol Pd_{surf}s). However, it was our intention to gain fundamental insight into the impact of the nature of the support on activity not on the activity as such.

Catalytic experiments were also conducted at different temperatures (225, 250, and 275 °C) to determine the apparent activation energies, and subsequently first order kinetics were applied. From the Arrhenius plots, as given in Figure 6, the apparent activation energies were calculated,

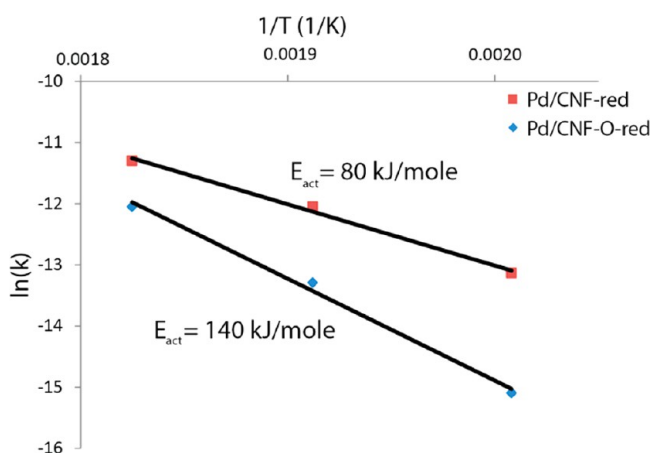


Figure 6. Arrhenius plots using first order reaction kinetics for the determination of the apparent activation energy. $P = 6 \text{ bar}$ N_2 , $m_{\text{stearic acid}} = 1 \text{ g}$, $m_{\text{cat}} = 0.25 \text{ g}$, $m_{\text{dodecane}} = 18 \text{ g}$.

resulting in a value of 140 kJ/mol for Pd/CNF-red and 80 kJ/mol for Pd/CNF-O-red. A significant lowering of the apparent activation energy is thus observed upon introducing oxygen containing groups on the support. This could indicate that different reaction pathways are followed for the different catalysts (see below).

Spent Catalyst Characterization. The oxygen containing groups present on the pristine catalyst might change during reaction as a result of the reaction conditions.^{15,16,19} Therefore we investigated the oxygen content for the spent catalysts by XPS and titration (Table 1). Pd/CNF-sp showed no change compared to Pd/CNF-red. It can thus be concluded that over the whole process, that is, activation and reaction, no significant change in oxygen content occurred for this catalyst. The remaining oxygen after the heat treatment at 625 °C is thus present as thermally stable groups, that is, ketonic, ether, and

phenolic groups.¹⁹ A minor change in the oxygen content is observed on going from Pd/CNF-O-red to Pd/CNF-O-sp upon reaction. The O/C ratio, obtained by XPS, decreased from 5.9×10^{-2} to 5.4×10^{-2} . Since Pd/CNF-O-red still contained acidic (carboxylic) groups as discussed above it is likely that these groups decomposed during the reaction as they are the least stable.¹⁵ This is confirmed by titration as Pd/CNF-O-sp did not reveal any acidic oxygen containing groups.

Additionally, particle sizes determined by XRD and TEM analysis of the spent catalysts showed no change in the average Pd particle sizes and remained at 7 nm during the catalytic experiments.

Influence of Oxygen Containing Groups on Catalysis. Based on the results given above it is concluded that the introduction of oxygen containing groups onto Pd/CNF is highly beneficial for the deoxygenation of stearic acid. The increasing oxygen content, and thereby increased support polarity, influences catalysis by modifying the mode of reactant adsorption, as has already been discussed in the Introduction. In the case of deoxygenation, the differences in polarity are speculated to lead to a different mode of adsorption of the amphiphilic fatty acid molecules onto the carbon surface as is schematically shown in Figure 7. At low polarity the apolar tail

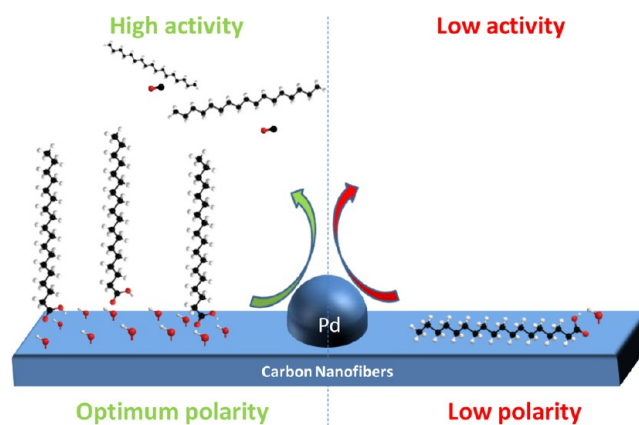


Figure 7. Schematic representation of the influence of oxygen containing groups on the deoxygenation of stearic acid.

is proposed to be preferentially adsorbed on the surface whereas in the case of high polarity this is the polar head, because of a hydrogen-bonding effect between the carboxylic group of the fatty acid and the oxygen containing groups on the support. Especially in the apolar solvent dodecane, these interactions are favored. As a result, a different orientation of fatty acid molecules is hypothesized on a more polar support surface, which could result in a larger concentration of these reactants on the support. We speculate that the reaction mainly occurs at the Pd-support perimeter. The interaction between the support oxygen containing groups and the carboxylic group of the fatty acid might also lead to activation of the latter and thereby facilitate the removal of this group in the presence of palladium, which would explain the observed lower activation energy. This hypothesis is comparable to the influence of oxygen containing groups on the catalytic oxidation of benzyl alcohol as proposed by Tang et al.,⁶ where it was reported that a higher amount of oxygen containing groups on the support resulted in a decreased interaction between the benzyl part of the reactant and the support and activation of the alcohol group. By altering the oxygen content one could thus propose

that the wettability of the support surface is varied, which significantly affects catalysis as also mentioned in the literature.²⁸ Alternatively, support polarity might lead to a higher heat of adsorption of the stearic acid, thereby lowering the apparent activation energy of the deoxygenation reaction. Also, the degree of freedom and the orientation for the fatty acid molecule is altered (Figure 7) by the introduction of oxygen groups. This results in a change in the entropy of adsorption which in turn will have an effect on the apparent activation free energy. Further research will be needed to obtain direct evidence for coverages and orientation of fatty acid molecules on catalyst surfaces.

CONCLUSIONS

Pd/CNF catalysts with a low and high support oxygen content but similar Pd particle size were successfully prepared. The latter samples were obtained by a gas phase oxidation of the former without changing the properties of the Pd. The catalysts with high oxygen content ($O/C = 5.9 \times 10^{-2}$ at/at) displayed a five times higher initial activity compared to the samples with low amounts of oxygen ($O/C = 3.5 \times 10^{-2}$ at/at).

The beneficial effect of oxygen containing groups on the carbon support is ascribed to an adsorption effect, that is, an increased interaction between the polar carboxylic group of the fatty acid and the support with a high polarity due to the oxygen containing groups. This is hypothesized to result in a preferential mode of adsorption of the fatty acids, that is, adsorbed with the carboxylic head on the support, and thereby a more facile decomposition at the palladium-support perimeter.

AUTHOR INFORMATION

Corresponding Author

*E-mail: J.H.Bitter@uu.nl. Phone: +31 6 227 36 131. Fax: +31 30 251 1027. Homepage: www.anorg.chem.uu.nl.

Notes

The authors declare no competing financial interest.

ACKNOWLEDGMENTS

This research has been performed within the framework of the CatchBio program. The authors gratefully acknowledge the support of the Smart Mix Program of The Netherlands Ministry of Economic Affairs and The Netherlands Ministry of Education, Culture and Science. Lucian Roiban and Hans Meeldijk are kindly acknowledged for TEM measurements, Stefan Hollak (Wageningen UR—Food and Biobased Research) for his help during the catalytic tests, and Joe Stewart for his assistance. Also, the authors express their gratitude to Frits van der Klis (Wageningen UR—Food and Biobased Research) for setting up the fatty acid analysis methods.

REFERENCES

- (1) Bitter, J. H.; Seshan, K.; Lercher, J. A. *J. Catal.* **1997**, *171*, 279–286.
- (2) Toebes, M. L.; Zhang, Y.; Hajek, J.; Nijhuis, A.; Bitter, J. H.; van Dillen, de Jong, K. P. *J. Catal.* **2004**, *226*, 215–225.
- (3) Wang, X.; Li, N.; Webb, J. A.; Pfefferle, L. D.; Haller, G. L. *Appl. Catal., B* **2010**, *101*, 21–30.
- (4) Armenise, S.; Roldán, L.; Marco, Y.; Monzón, A.; García-Bordejé, J. *Phys. Chem. C* **2012**, *116*, 26385–26395.
- (5) Plomp, A. J.; Vuori, H.; Krause, A. O. I.; de Jong, K. P.; Bitter, J. H. *Appl. Catal., A* **2008**, *351*, 9–15.

- (6) Tang, T.; Yin, C.; Xiao, N.; Guo, M.; Xiao, F. S. *Catal. Lett.* **2009**, *127*, 400–405.
- (7) Huber, G. W.; Iborra, S.; Corma, A. *Catal. Rev.* **2006**, *106*, 4044.
- (8) Abhilash, P. C.; Srivastava, P.; Jamil, S.; Singh, N. *Environ. Sci. Pollut. Res.* **2011**, *127*.
- (9) Juan, J. C.; Kartika, D. A.; Wub, T. Y.; Hin, T.-Y. *Bioresour. Technol.* **2011**, *102*, 452.
- (10) van Gerpen, J.; Shanks, B.; Pruszko, R.; Clements, D.; Shanks, B.; Pruszko, R.; Clements, D.; Knothe, G.; *Biodiesel Production Technology Aug. 2002–Jan. 2004*; <http://www.nrel.gov/docs/fY04osti/36244.pdf>.
- (11) Snåre, M.; Kubičková, I.; Mäki-Arvela, P.; Eränen, K.; Murzin, D. Y. *Ind. Eng. Chem. Res.* **2006**, *45*, 5708–5715.
- (12) Kubičková, I.; Snåre, M.; Eränen, K.; Mäki-Arvela, P.; Murzin, D. Y. *Catal. Today* **2005**, *106*, 197–200.
- (13) Morgan, T.; Grubb, D.; Santillan-Jimenez, E.; Crocker, M. *Top. Catal.* **2010**, *53*, 820–829.
- (14) Ping, E. W.; Pierson, J.; Wallace, R.; Miller, J. T.; Fuller, T. F.; Jones, C. W. *Appl. Catal., A* **2011**, *396*, 85–90.
- (15) Gosselink, R. W.; van den Berg, R.; Xia, W.; Muhler, M.; de Jong, K. P.; Bitter, J. H. *Carbon* **2012**, *50*, 4424–4431.
- (16) Xia, W.; Jin, C.; Kundu, S.; Muhler, M. *Carbon* **2009**, *47*, 919–922.
- (17) Briggs, D.; Seah, M. P., Eds.; *Practical surface analysis*; John Wiley and Sons: New York, 1994; pp 635–638.
- (18) Butte, W. *J. Chromatogr.* **1983**, *261*, 142–145.
- (19) Kundu, S.; Wang, Y.; Xia, W.; Muhler, M. *J. Phys. Chem. C* **2008**, *112*, 16869–16878.
- (20) Wagemans, R. *Magnesium for Hydrogen Storage*. Ph.D. Thesis, Utrecht University, The Netherlands, Chapter 6.
- (21) Mojet, B. L.; Kappers, M. J.; Muijsers, J. C.; Niemantsverdriet, J. W.; Miller, J. T.; Modica, F. S.; Koningsberger, D. C. *Stud. Surf. Sci. Catal.* **1994**, *84*, 906–916.
- (22) Toyoshima, R.; Yoshida, M.; Monya, Y.; Kousa, Y.; Suzuki, K.; Abe, H.; Mun, B. S.; Mase, K.; Amemiya, K.; Kondoh, H. *J. Phys. Chem. C* **2012**, *116*, 18691–18697.
- (23) Hollak, S. A. W.; Bitter, J. H.; van Haveren, J.; de Jong, K. P.; van Es, D. S. *RSC Adv.* **2012**, *2*, 9387–9391.
- (24) Smits, G. *J. Am. Oil Chem. Soc.* **1976**, *53*, 122.
- (25) Lestari, S.; Simakova, I.; Tokarev, A.; Mäki-Arvela, P.; Eränen, K.; Murzin, D. Y. *Catal. Lett.* **2008**, *122*, 247–251.
- (26) Bernas, H.; Eränen, K.; Simakova, I.; Leino, A.-R.; Kordás, K.; Myllyoja, J.; Mäki-Arvela, P.; Salmi, T.; Murzin, D. Y. *Fuel* **2010**, *89*, 2033–2039.
- (27) Mäki-Arvela, P.; Snåre, M.; Eränen, K.; Myllyoja, J.; Murzin, D. Y. *Fuel* **2008**, *87*, 3543–3549.
- (28) Liu, F.; Wang, L.; Sun, Q.; Zhu, L.; Meng, X.; Xiao, F.-S. *J. Am. Chem. Soc.* **2012**, *134*, 16948.